

P 18

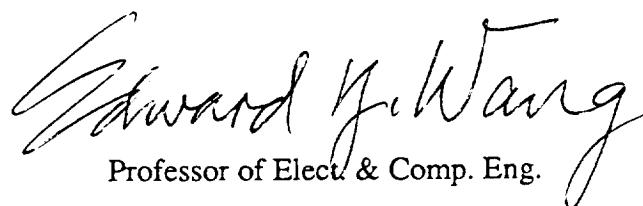
IN-44-12



Final Technical Report of
NASA - ASU Internship Program
(NAG 3-383)

Submitted by

Dr. Edward Y. Wang



Professor of Elect. & Comp. Eng.

Arizona State University

Tempe, Arizona 85287

October 27, 1989

(NASA-CR-185996) THE PHOTOVOLTAIC
PROPERTIES OF AN Al In As/InP
HETEROJUNCTIONS GROWN BY LPE METHOD Final
Technical Report (Arizona State Univ.)
18 p

N90-13586

Unclass
0239259

CSCL 10A G3/44

FINAL REPORT

NASA-ASU INTERNSHIP PROGRAM

The objectives of the NASA-ASU Internship Program is to train students in the general area of solar cell research. There have been two students on the NASA-ASU internship, Mr. John Donahue and Mr. Shao-Wen Hsia. John Donahue graduated with a Ph.D in Dec. 1986. The title of his dissertation is "Excitation of the Radiative Surface Plasmons Mode in Metal-Oxide-Metal Tunnel Junctions. Part of his experimental work was carried out in the NASA-Lewis Center. As a result of his research two journal articles were published in the Journal of Applied Physics. Reprints of the two articles are attached as part of the final report.

Mr. Hsia was on the internship program for the past year and a half. His research is mainly in the are of $Al_x In_{1-x}As/InP$ heterojunction solar cell studies. Those heterojunction solar cells were fabricated by LPE method. A technical report of his work is also attached in the final report.

THE PHOTOVOLTAIC PROPERTIES OF AL IN AS/INP HETEROJUNCTIONS GROWN BY LPE METHOD

INTRODUCTION

$\text{Al}_{0.48}\text{In}_{0.52}\text{As}$ can be lattice-matched to InP and has a larger band gap than that of InP. It is a potential material for the fabrication of cascade solar cells. In this report, we will present some preliminary results of N/P and P/N $\text{Al}_{0.48}\text{In}_{0.52}\text{As}/\text{InP}$ heterojunction solar cells by the LPE method. Sn and Te are used for N-dopants and Zn for P-dopant in $\text{Al}_{0.48}\text{In}_{0.52}\text{As}$ epilayers. Photoluminescence[PL], current-voltage[I-V] in dark and under light illuminations, and capacitance-voltage[C-V] are utilized in our studies. PL results provide the evidence of $\text{Al}_{0.48}\text{In}_{0.52}\text{As}$ epilayer on InP substrate. I-V measurements suggest that recombination centers dominate the current conduction mechanism and the high series-resistance [5-60 ohm] exists with the heterojunctions. C-V results indicate that the Te-doped N/P is an abrupt junction while Sn-doped N/P is a linear junction. The best conversion efficiency of these heterojunction solar cells is estimated at about 5%. Therefore, based on our results, we conclude that considerable improvements are needed in how to grow thick epilayer and how to reduce the series-resistance in order to compete with the conventional Si, GaAs, and InP homojunction solar cells.

EXPERIMENT

A horizontal sliding LPE system was used to grow $\text{Al}_x\text{In}_{1-x}\text{As}$ epilayers on N and P InP substrates. The heterojunction structures of N/P and P/N solar cells are shown in Figure 1. The growth from ternary liquid solutions is based on the results of K. Nakajima et al.¹ Materials were semiconductor-grade Al, In, Te, Zn, InP polycrystal, and InAs polycrystal. K Nakajima et al.^{2,3,4} used AlIn mother alloy which contained 0.1 at % Al for Al source. It was very difficult to dissolve Al, melts directly at the growth temperatures because of the miscibility gap in the liquid state of the Al and In binary system. The lattice-matched ternary epilayer can be grown starting from 777°C using the solution composition of $X_{\text{Al}}^1 = 0.00066$, $X_{\text{As}}^1 = 0.142$ and $X_{\text{In}}^1 =$

0.85734. In our experiment, we put In and Al in the same graphite bin with weight ratio 4612:1. They were baked at 810°C in purified H₂ flow for 16 hrs. After the baking process, the InAs polycrystal and X¹_{Te} = 2.53478E-4 or X¹_{Zn} = 3.2957E-5 were added to AlIn solution. The weight ratio between Al and InAs polycrystal was 1:1513. The whole material were baked again at 810°C for 30 min and cooled down with a constant cooling rate 20-30C/h. The starting growth temperature for AlInAs was 770°C. The accurate supercooling temperature was not clear because of lack of phase diagram. The growth time intervals ranged from 7 min. to 34 min. and the thickness changed from 165nm to 375nm. The growth rate of Al_xIn_{1-x}As was quite small, which was about 22nm/min. The epilayer thickness was not linearly proportional to the growth time beyond 20 minutes growth because of the depletion of Al in the melt. Low temperature photoluminescence (PL), I-V, and C-V measurements were carried out to characterize Al_xIn_{1-x}As/InP heterojunction diodes.

After the growth process, ohmic contacts were made on both sides of the substrate and epilayers. Lithography and lift-off were used to make a mesa-type diode with front grid contacts on epilayers. The P-type contact consisted of 10 wt.% Sn in Au alloy and N-type contacts had 10 wt.% of Zn in Au alloy. Metal contacts were thermally evaporated to about 400nm., then samples were alloyed at 260°C for 3 min. in 10% H₂ forming gas to obtain good ohmic contacts. The area of each diode was 2x2 mm² without epoxy encapsulation and and antireflection coating.

RESULTS AND DISCUSSIONS

I. PHOTOLUMINESCENCE MEASUREMENTS

Photoluminescence is commonly used to analyze the properties of the semiconductor materials. The band gap of Al_xIn_{1-x}As (1.56eV at 4K) varied linearly with x for 0.45 < x < 0.55. For x = 0.463 peak at 1.48eV corresponds to the acceptor-band transition and the peak at 1.408eV (at 77°K) as shown in Fig. 2 was the direct transition between valence and conduction band. The band gap would be 1.506eV at 4°K as shown in Fig. 3, if the band gap changes linearly with the

temperature. The band gap is a little smaller than the ideal one. This might be due to aluminum exposure to the air during the processing and forming oxide on the surface, so the the aluminum composition was less than the required quantities in the solution. The band gap was smaller than 1.563eV (at 2K) for $x < 0.48$ and larger than that for $x > 0.48$. Quantum efficiencies of both structures were very low, with maximum values of the 14%. the profiles were different for these two structures, as shown in Fig. 4 and 5. P/N $\text{Al}_x \text{In}_{1-x} \text{As}/\text{InP}$ diode had a steeper rise at wavelength 915nm. The junction depth was much larger than that of the N/P diode and the exact P/N junction was located beyond the epilayer due to a larger diffusing coefficient of Zinc in the growth. AlInAs/InP (N/P) was not so sharp as the P/N one. Its maximum was located at 845nm, which corresponds to the AlInAs band gap. It had a slow rise starting from 915nm. This is due to photons penetrating through the ternary epilayer and generating electron-hole pairs in the InP.

II. CURRENT-VOLTAGE MEASUREMENT

Figure 6 and 7 give a semi-log plot of the current-voltage relationship for N/P and P/N heterojunctions. The forward current is found to be exponentially dependent on biased voltage over several decades of currents. The standard empirical representation of the current-voltage relationship is given by

$$I_f \sim I_0 (e^{qV_f/nkT} - 1)$$

where the ideality factor $n = 1$ for pure thermionic emission or diffusion current and $n = 2$ for pure recombination current. V_f is forward bias voltage. The thermionic emission current is more likely to be dominant for narrow band gap materials with low trap density at a high temperature, while the generation-recombination current tends to be dominant for large band gap materials at a low temperature. When both current components are comparable, n takes on value between 1 and 2. LPE grown $\text{Al}_{0.48}\text{In}_{0.52}\text{As}$ has band gap 1.45eV at room temperature, such that the recombination component usually is important to the current. The ideality factors of $\text{Al}_x \text{In}_{1-x} \text{As}/\text{InP}$ (N/P) diodes were about 1.3, while they were about 2 for $\text{Al}_x \text{In}_{1-x} \text{As}/\text{InP}$ (P/N) diodes. The J_0 was on the order of $\sim 10^{-9}$ - 10^{-10} A/cm², which was large for AlInAs/InP diodes.

III. CAPACITANCE-VOLTAGE

From C-V results, we have found the built-in voltages to be 1.2 volts by extrapolation for Te-doped N/P heterojunction as shown in Figure 10. The slope of $1/C^2$ vs. V yields carrier concentration for 10^{17} for $Al_{0.48}In_{0.52}As$ epilayer and $3.3 \times 10^{15}/cm^3$ for InP epilayer. For Sn-doped N/P heterojunction, C-V results is shown in Figure 11. $1/C^3$ vs. V plots yield a linear junction characteristics. Based on C-V results, we conclude that Sn-dopand in $Al_xIn_{1-x}As$ epilayer provides a non-uniform doping while Te-dopand gives a reasonable uniform carrier concentration during the LPE growth. No reproducible C-V results can be obtained on $Al_xIn_{1-x}As/InP$ (P/N) because of the high density of the recombination center and high series resistance in P/N heterojunctions.

CONCLUSIONS

We have successfully fabricated N/P and P/N $Al_{0.48}In_{0.52}As/InP$ heterojunction solar cells. The conversion efficiency of these solar cells is about 5%. In order to improve the conversion efficiency, we must develop a growth technique to produce thick (optimum) $Al_{0.48}In_{0.52}As$ epilayers. Density of recombination center should also be reduced to give a smaller saturation current, hence a larger open-circuit voltage.

REFERENCES

1. Kazuo Nakajima, Toshiyuki Tanahashi, and Kenzo Akita "Liquid Phase EPITAXIAL Growth of Lattice-matched $Al_{0.48}In_{0.52}As$ on InP." *Appl. Phys. Lett.* **41**(2) 15 July 1982, p. 194.
2. Kazuo Nakajima and Kenzo Akita, "Calculation of the Al-Ga-In-As Phase Diagram and LPE Growth of $Al_xGayIn_{1-x-y}As$ on InP." *Journal of Xtal Growth*, **54**, 1981, p. 232-238.
3. K. Nakajima, T. Tanahashi, S. Komiya, and K. Akita. "Liquid Phase Epitaxial Growth of $Al_xGayIn_{1-x-y}As$ on InP," *Journal of Xtal Growth*, **54**, 1981, p. 232-238.
4. G.A. Antypas, "Prevention of InP Surface Decomposition in Liquid Phase Epitaxial Growth." *Appl. Phys. Lett.* **37**(1), July 1980, p. 64

- Figure 1. Heterojunction Solar Cell Structures of $\text{Al}_{0.48}\text{In}_{0.52}\text{As}/\text{InP}$
- Figure 2. Photoluminescence at 77°K
- Figure 3. Photoluminescence at 4.2°K
- Figure 4. Spectral Response of $\text{Al}_{0.48}\text{In}_{0.52}\text{As}/\text{InP}$ (P/N) Solar Cells.
- Figure 5. Spectral Response of $\text{Al}_{0.48}\text{In}_{0.52}\text{As}/\text{InP}$ (N/P) Solar Cells.
- Figure 6. Semilog Plot of the Current-Voltage Relationship for N/P Heterojunction.
- Figure 7. Semilog Plot of the Current-Voltage Relationship for P/N Heterojunction.
- Figure 8. Linear Plot of the Current-Voltage Relationship for N/P Heterojunction.
- Figure 9. Linear Plot of the Current-Voltage Relationship for P/N Heterojunction.
- Figure 10. $\frac{1}{C^2}$ vs. V. plot for the Te-doped N/P Heterojunction.
- Figure 11. $\frac{1}{C^3}$ vs. V. plot for the Sn-doped N/P Heterojunction.

- Figure 1. Heterojunction Solar Cell Structures of $\text{Al}_{0.48}\text{In}_{0.52}\text{As}/\text{InP}$
- Figure 2. Photoluminescence at 77°K
- Figure 3. Photoluminescence at 4.2°K
- Figure 4. Spectral Response of $\text{Al}_{0.48}\text{In}_{0.52}\text{As}/\text{InP}$ (P/N) Solar Cells.
- Figure 5. Spectral Response of $\text{Al}_{0.48}\text{In}_{0.52}\text{As}/\text{InP}$ (N/P) Solar Cells.
- Figure 6. Semilog Plot of the Current-Voltage Relationship for N/P Heterojunction.
- Figure 7. Semilog Plot of the Current-Voltage Relationship for P/N Heterojunction.
- Figure 8. Linear Plot of the Current-Voltage Relationship for N/P Heterojunction.
- Figure 9. Linear Plot of the Current-Voltage Relationship for P/N Heterojunction.
- Figure 10. $\frac{1}{C^2}$ vs. V. plot for the Te-doped N/P Heterojunction.
- Figure 11. $\frac{1}{C^3}$ vs. V. plot for the Sn-doped N/P Heterojunction.

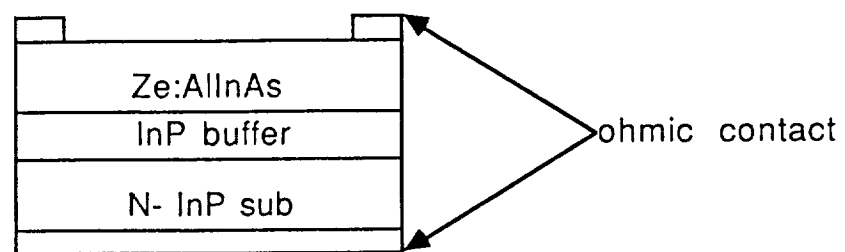
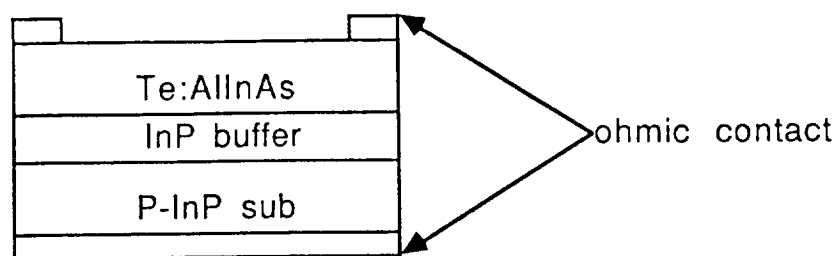


FIGURE 1

H23. PL1

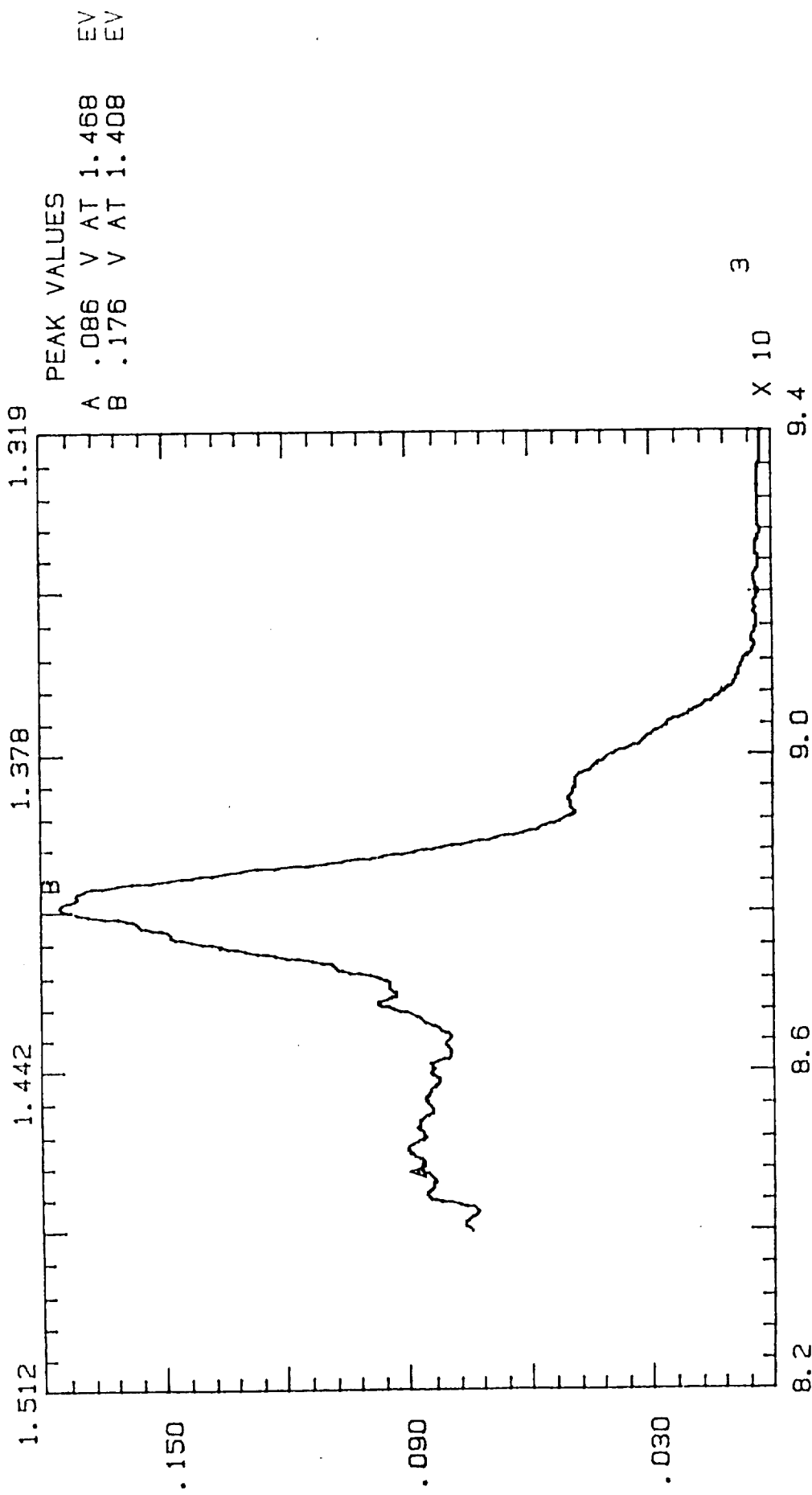


FIGURE 2

RON11.PL1

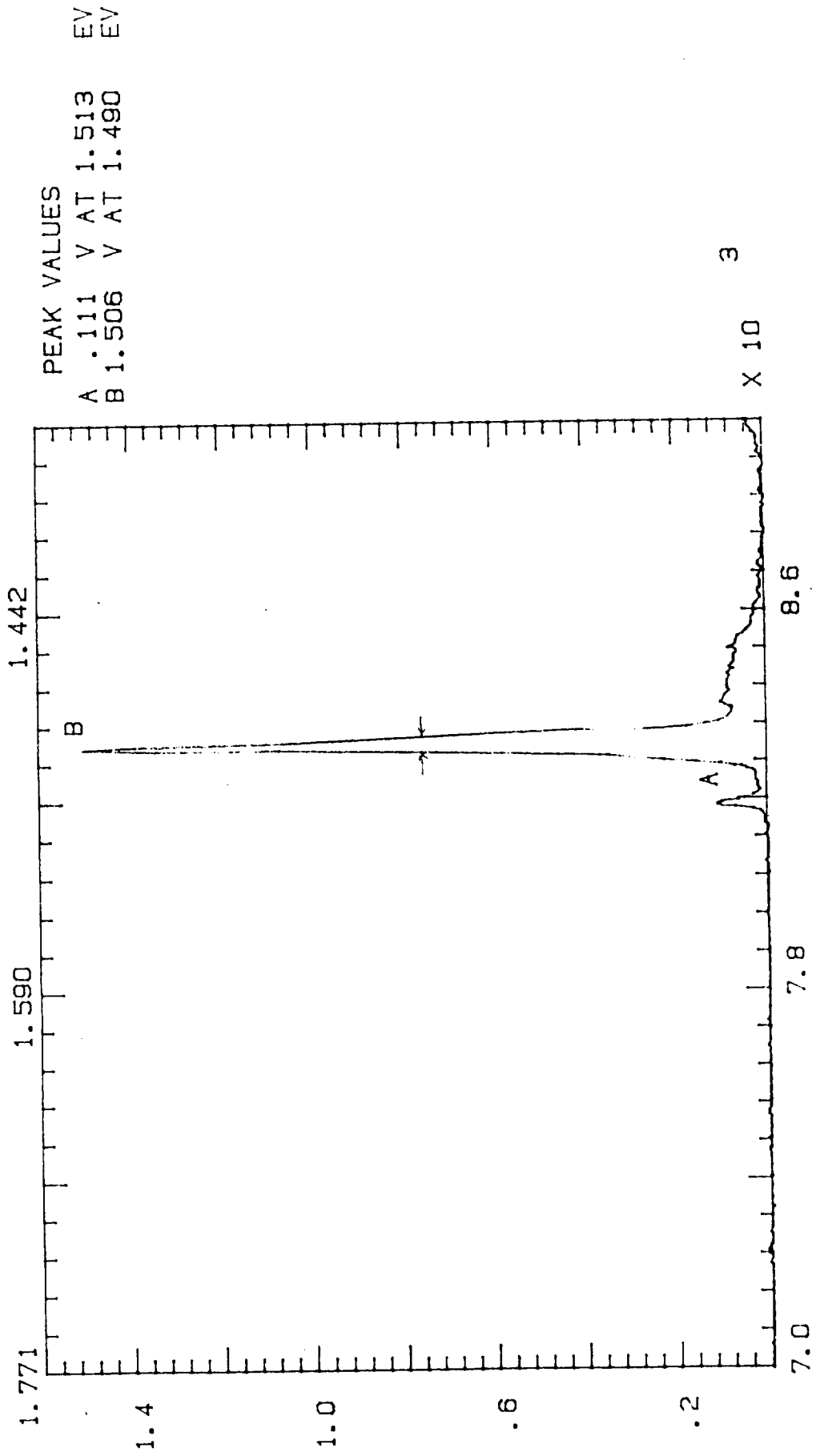


FIGURE 3

FIGURE 4

23-A

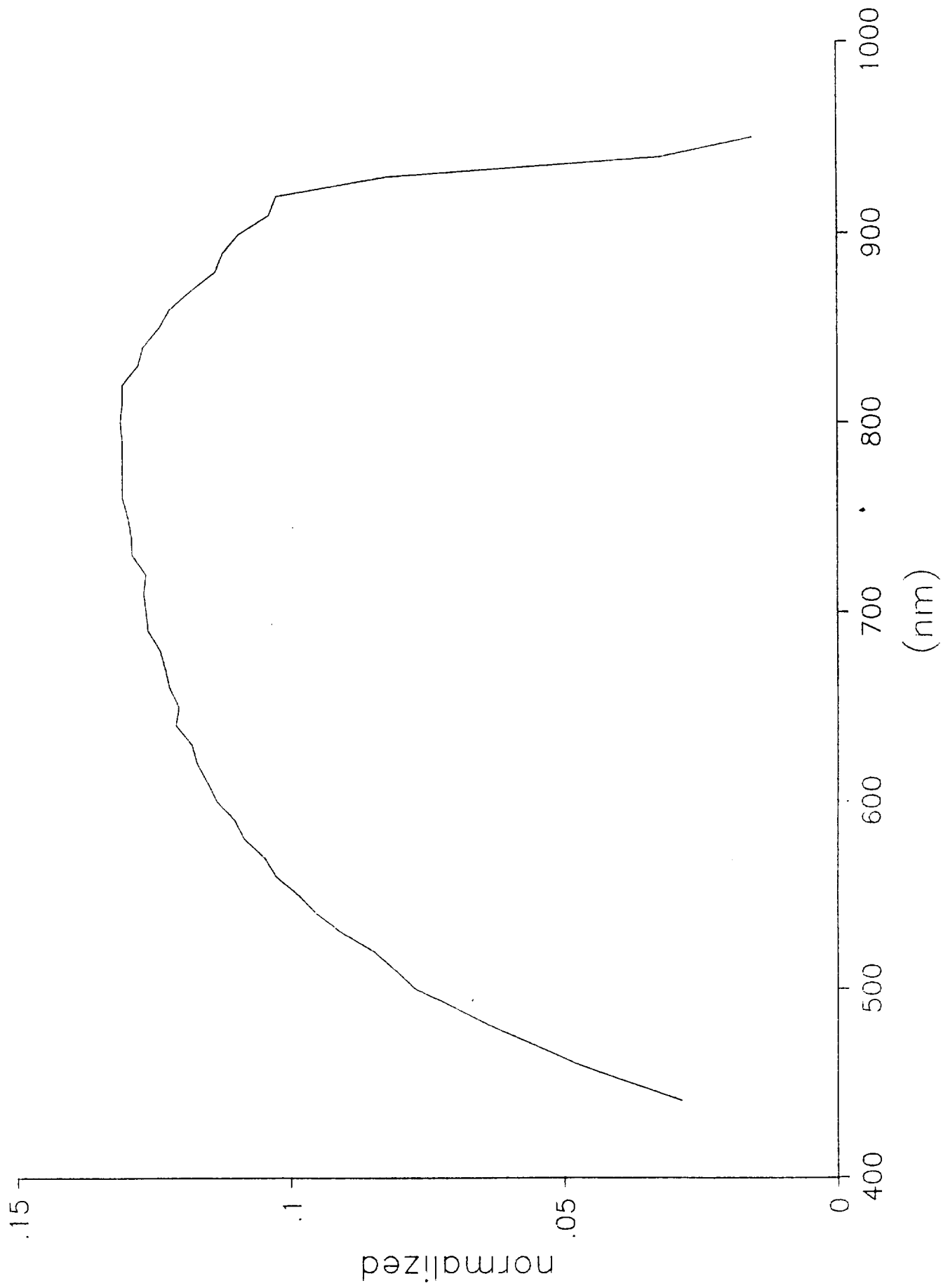


FIGURE 5

17-B

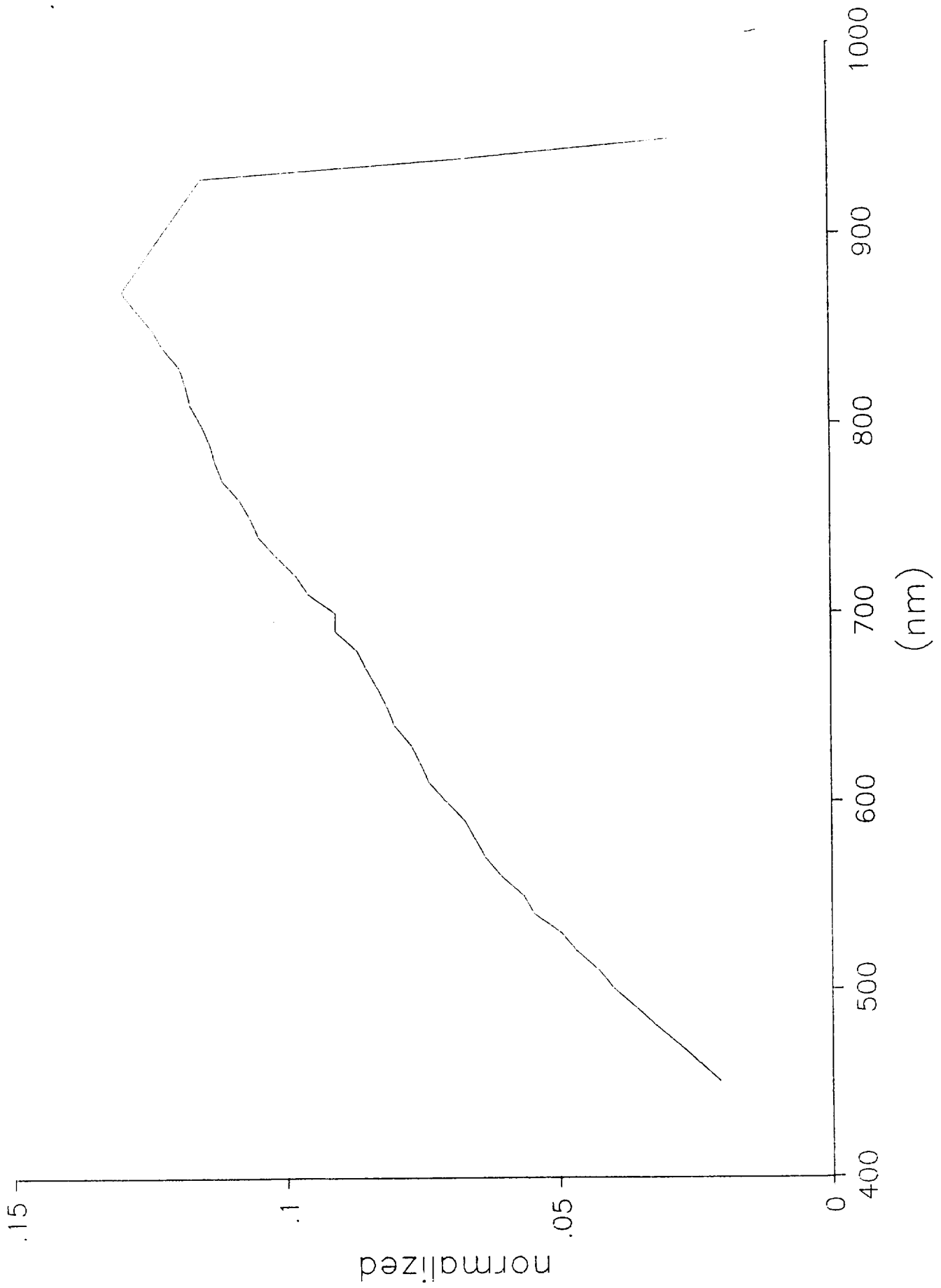
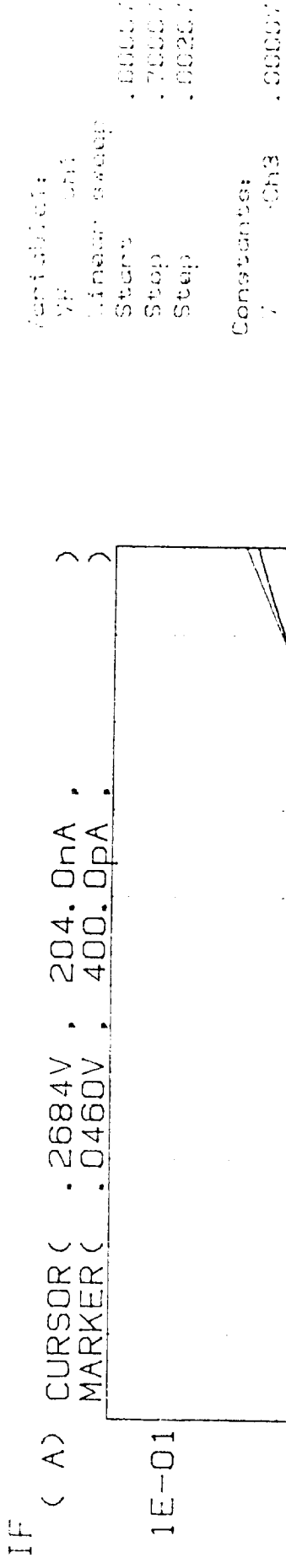


FIGURE 6

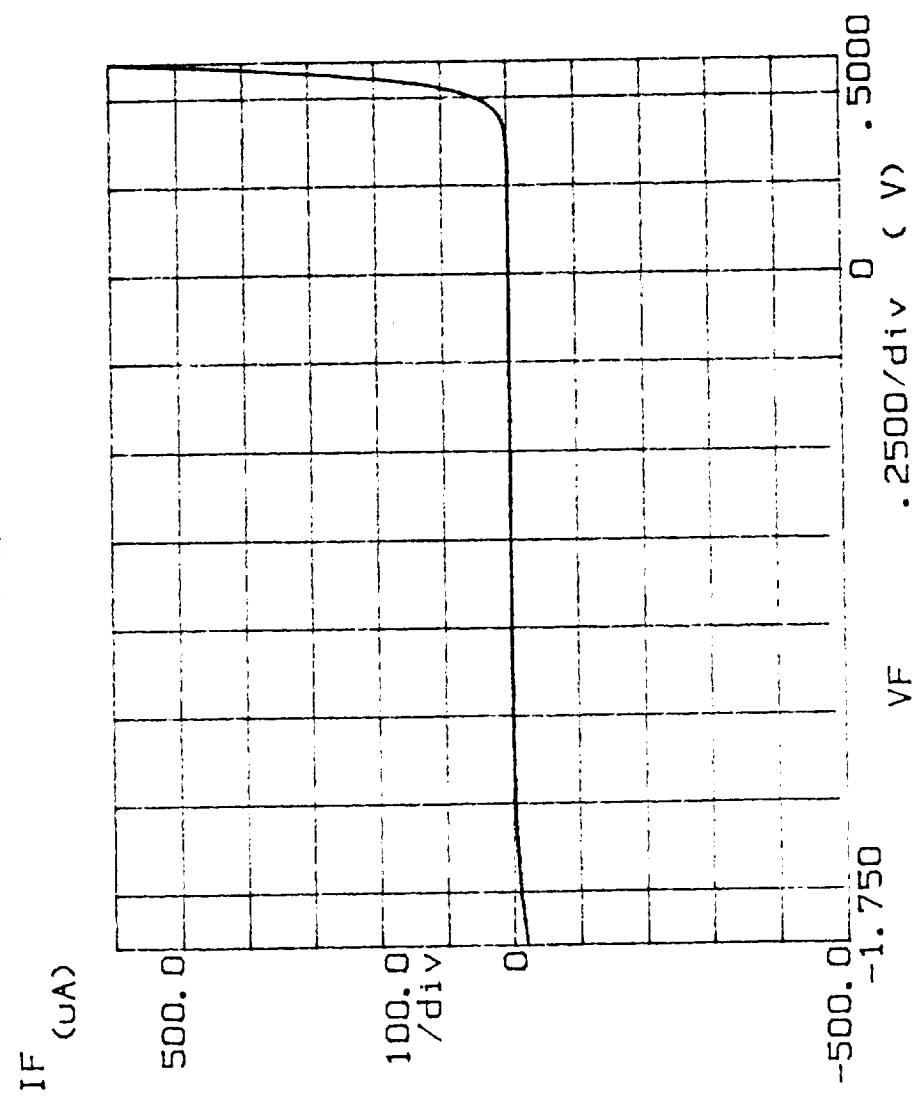
***** GRAPHICS PLOT *****



ORIGINAL PAGE IS
 OF POOR QUALITY

| LINE1 | GRAD | 1/GRAD | Xintercept | Yintercept |
|-------|----------|----------|------------|------------|
| LINE2 | 10.3E+00 | 97.3E-03 | 920E-03 | 357E-12 |

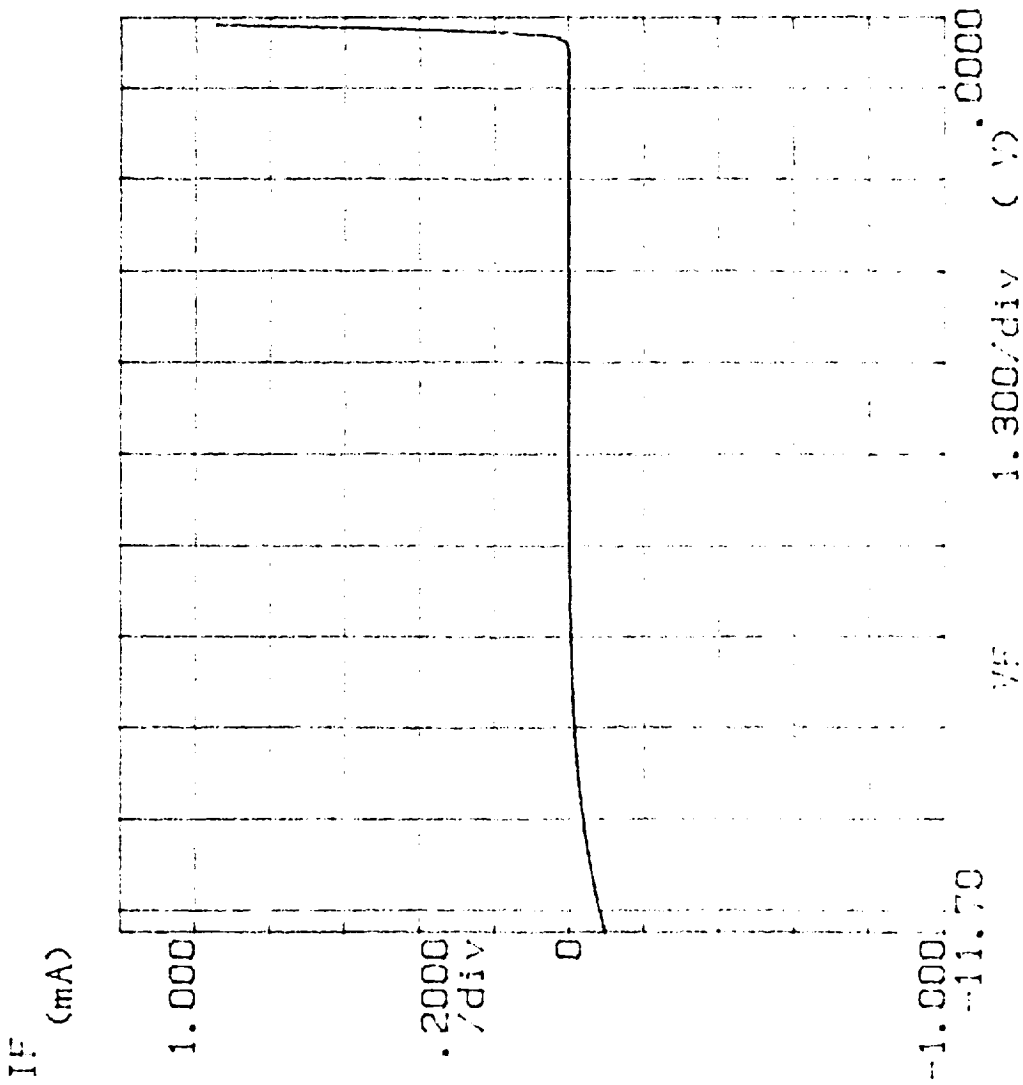
***** GRAPHICS PLOT *****
 ND. 23-7 SOLAR CELL 2/24



Variable:
 VF -Ch1
 Linear sweep
 Start -1.9000V
 Stop .8000V
 Step .0050V
 Constant:
 V -Ch3 .0000V

FIGURE 8

***** GRAPHICS PLOT *****



Variables:
 VF -Ch1
 Linear sweep
 Start -12.000V
 Stop 1.0000V
 Step .0500V
 Constant:
 Y -Ch3 .0000V

ORIGINAL PAGE IS
 OF POOR QUALITY

FIGURE 9

FIGURE II

12-1 1/C³-V PLOT

